Regulation of nonmuscle myosin II during 3-methylcholanthrene induced dedifferentiation of C2C12 myotubes

ARTICLE *in* EXPERIMENTAL CELL RESEARCH · MAY 2014

Impact Factor: 3.25 · DOI: 10.1016/j.yexcr.2014.05.015 · Source: PubMed

5 AUTHORS, INCLUDING:

Mahua Das
Indian Association for the Cultivation of Sci…
8 PUBLICATIONS **65** CITATIONS
SEE PROFILE

Siddhartha Jana
Indian Association for the Cultivation of Sci…
27 PUBLICATIONS **547** CITATIONS
SEE PROFILE

EXPERIMENTAL CELL RESEARCH 326 (2014) 68–77

Available online at www.sciencedirect.com

ScienceDirect

journal homepage: www.elsevier.com/locate/yexcr

Research Article

Regulation of nonmuscle myosin II during 3-methylcholanthrene induced dedifferentiation of C2C12 myotubes

*Sumit K. Dey, Shekhar Saha, Provas Das, Mahua R. Das, Siddhartha S. Jana**

Department of Biological Chemistry, Indian Association for the Cultivation of Science, Jadavpur, Kolkata 32, India

ARTICLE INFORMATION

Article Chronology:
Received 17 February 2014
Received in revised form
19 May 2014
Accepted 20 May 2014
Available online 2 June 2014

Keywords:
Myotubes
Nonmuscle myosin II
Fragmentation
Dedifferentiation
3-Methylcholanthrene
Myosin regulatory light chain

ABSTRACT

3-Methylcholanthrene (3MC) induces tumor formation at the site of injection in the hind leg of mice within 110 days. Recent reports reveal that the transformation of normal muscle cells to atypical cells is one of the causes for tumor formation, however the molecular mechanism behind this process is not well understood. Here, we show in an in vitro study that 3MC induces fragmentation of multinucleate myotubes into viable mononucleates. These mononucleates form colonies when they are seeded into soft agar, indicative of cellular transformation. Immunoblot analysis reveals that phosphorylation of myosin regulatory light chain (RLC_{20}) is 5.6±0.5 fold reduced in 3MC treated myotubes in comparison to vehicle treated myotubes during the fragmentation of myotubes. In contrast, levels of myogenic factors such as MyoD, Myogenin and cell cycle regulators such as Cyclin D, Cyclin E1 remain unchanged as assessed by real-time PCR array and reverse transcriptase PCR analysis, respectively. Interestingly, addition of the myosin light chain kinase inhibitor, ML-7, enhances the fragmentation, whereas phosphatase inhibitor perturbs the 3MC induced fragmentation of myotubes. These results suggest that decrease in RLC_{20} phosphorylation may be associated with the fragmentation step of dedifferentiation.

Introduction

The polycyclic aromatic hydrocarbon, 3-Methylcholanthrene (3MC), induces tumor formation in humans and other living organisms [1]. Several studies have revealed that 3MC exerts most of its tumorigenic effect by introducing mutations in genes such as *ras* and p53 [2,3], which promote cell proliferation, and by modulating structural changes in DNA such as perturbation in vertical nucleotide stacking and the phosphodiester-deoxyribose backbone [4,5]. These mutations in *ras* and p53, and structural changes in DNA are expected to influence gene expression and the fidelity of replication and transcription, having a pivotal effect on the neoplastic transformation of normal tissue [6–9].

A 3MC-induced mouse tumor is a model system for studying the molecular mechanism behind the development of tumors. Koebel et al. [10] showed that cellular transformation of fibroblast-like

Abbreviations: 3MC, 3-Methylcholanthrene; NM II, nonmuscle myosin II; NMHC, nonmuscle myosin heavy chain; GM, growth medium; DM, differentiation medium; RLC_{20}, regulatory light chain; DMEM, Dulbecco's Modified Eagle's Medium; BrdU, 5-bromo-2′-deoxyuridine

**Corresponding author.* Fax: +91 33 2483 6561.
E-mail addresses: bcssj@iacs.res.in, siddhartha.jana@gmail.com (S. S. Jana).

http://dx.doi.org/10.1016/j.yexcr.2014.05.015
0014-4827/

cells to atypical cells, which were characterized by enlarged vesicular nuclei, prominent nucleoli and heterogeneous morphologies, was one of the causes for the formation of tumor in the 3MC-induced mouse tumor model. Recently, Saha et al. [11] have established an in vitro system, in which 3MC was shown to initiate fragmentation in C2C12 myotubes. However, the mechanism behind 3MC induced fragmentation in C2C12 myotube is yet to be understood.

C2C12 myotubes are formed from the fusion of C2C12 myoblasts in a linear fashion [12]. Swailes et al. [13] have reported that nonmuscle myosin IIs (NM IIs) drive myoblasts to align and fuse to form multinucleated myotubes. Both NM II-A and -II-B are found to be localized in the Z-line and intercalated disc of human skeletal muscle, suggesting a possible role in the contraction/relaxation mechanism of skeletal muscle [14,15]. But, their role in the reversion of terminally differentiated myotubes to mononucleated cells is not known. NM IIs are actin based motor proteins which play important role in cytokinesis, migration, and wound closure after tissue injury [16–18]. NM IIs are composed of two heavy chains of 230 kDa, two regulatory light chains (RLC_{20}) and two essential light chains (ELC_{17}). Three different genes: *MYH9*, *MYH10*, and *MYH14* code for three isoforms of nonmuscle myosin heavy chain (NMHC) II-A, -II-B, and -II-C, respectively in mammals [19]. Recently, three different isoforms of the RLC_{20} have been identified in mammals both at transcript and protein levels, giving rise to complexity of NM II biology [20]. Enzymatic activity of these NM IIs is regulated by phosphorylation and dephosphorylation of RLC_{20} which are catalyzed by enzymes such as myosin light chain kinase (MLCK), Rho kinase and myosin phosphatase [21–24].

In this study, we have shown that 3MC reduces the phosphorylation of RLC_{20} during the fragmentation step of dedifferentiation in C2C12 myotubes. Also, reduction of RLC_{20} phosphorylation by myosin light chain kinase inhibitor, ML-7, induces C2C12 myotube fragmentation whereas inhibition of 3MC-mediated loss of RLC_{20} phosphorylation by phosphatase inhibitor delays fragmentation, suggesting a relationship between RLC_{20} phosphorylation and myotube fragmentation.

Materials and methods

Cell culture, differentiation and dedifferentiation

A mouse C2C12 myoblast cell line (ATCC, Manassas, VA, USA) was grown in growth medium (GM): Dulbecco's modified Eagle's medium (DMEM from Life Technologies, Carlsbad, CA, USA) containing 10% fetal bovine serum, 100 units/ml penicillin, 100 μg/ml streptomycin in a 5% CO_2 incubator at 37 °C. To initiate differentiation, C2C12 cells were allowed to reach 80% confluency, and growth medium was replaced with differentiation medium (DM): DMEM containing 2% horse serum, 100 units/ml penicillin, 100 μg/ml streptomycin. After 3–4 days, 50–60% of myoblasts form myotubes as determined by DAPI staining.

We isolated myotubes from the culture according to Frangini et al. [25]. Briefly, cells were treated with 0.05% trypsin-EDTA for 5 min and the dish was tilted up and down. The detached cells, mostly myotubes, were resuspended in fresh DM and plated in a new culture dish. After 30 min, the floating myotubes were transferred to a second culture dish. The medium was replaced with fresh DM after 6–12 h when the myotubes were attached. Any mononucleated cells that settled on the dishes were removed with a needle [26].

Purified myotubes were treated with 0–50 nM 3MC, Phosphatase inhibitor cocktail 1 (2 μl/ml [27], Sigma-Aldrich, St. Louis, MO, USA) with 50 nM 3MC, ML-7 (10 μM [28], Sigma-Aldrich), or 0.0001–0.1% DMSO (vehicle control) for another 1–3 days. Medium was replaced with DM containing the same concentration of drugs or vehicle at 24 h intervals. Images were captured using an Olympus IX-51 microscope (Tokyo, Japan).

Soft agar colony assay

According to a previously published protocol [29], we prepared 0.5% base agar in DMEM media supplemented with 10% FBS and kept at 37 °C for an hour in a 35 mm culture dish. Mononucleated cells derived from 50 nM 3MC treated myotubes were suspended in 0.3% agarose in the same media and plated on the top of the base agar and allowed to grow for 20–30 days in a 37 °C and 5% CO_2 incubator. Cells were fed with fresh GM at one week intervals. Images were captured using Olympus IX-51 microscope at 7 day intervals.

Electrophoresis, immunoblot and immunostaining

Cell lysates from treated and untreated C2C12 myotubes were prepared as previously published [11]. Briefly, cells were washed with cold phosphate buffer saline (PBS) and directly lysed with Laemmli sample buffer. Then, the samples were run on 8% SDS-PAGE, followed by transfer to a polyvinylidene difluoride membrane (Millipore Corporation, Billerica, MA, USA). The membrane was blocked for 1 h at room temperature with 5% nonfat milk or 5% bovine serum albumin (BSA), 0.05% Tween-20 in phosphate buffer saline. Then the upper part of the membrane was incubated with antibodies to MyoD (1:800, Santa Cruz Biotechnology Inc., Santa Cruz, CA, USA), Myogenin (1:800, Santa Cruz Biotechnology), or p-Ser-1943 (1:2000, Cell Signaling Technology, Danvers, USA) and the lower part with antibodies to regulatory light chain (RLC_{20}, 1:2000, Cell Signaling), Phospho-Ser19 RLC_{20} (p-RLC_{20}, 1:5000, Cell Signaling) or GAPDH, (1:5000, Santa Cruz Biotechnology Inc.) overnight at 4 °C. The membrane was washed and incubated with horseradish-peroxidase-conjugated secondary antibody at room temperature for 2 h and developed by Super Signal West Femto reagent (Thermo Fisher Scientific Inc. Waltham, MA, USA). Relative band intensity was quantified using ImageJ software (NIH, Bethesda, MD, USA) after normalizing with GAPDH or RLC_{20} band intensity.

For immunostaining, cells were fixed with 4% paraformaldehyde at room temperature for 30 min, permeabilized with 0.1% Triton X-100 in PBS for 10 min, blocked with 0.05% Triton X-100 and 2% BSA in PBS for 1 h. Cells were then incubated with polyclonal antibodies against NMHC II-A or NMHC II-B (1:500, Cell Signaling) overnight at 4 °C. Alexa-594 tagged goat anti-rabbit IgG (1:500, Life Technologies) was used as secondary antibody at room temperature for 1 h. DAPI was added for 10 min to stain nuclei. After washing, samples were mounted with Prolong gold antifade reagent (Life Technologies). The images were captured using C1 confocal microscope (Nikon, Tokyo, Japan).

BrdU labeling

C2C12 myoblasts and the purified myotubes were labeled with BrdU (BD Bioscience, San Jose, CA, USA) as previously published [30]. Briefly, cells were treated with BrdU at a final concentration of 10 μM for 24 h in the presence of 50 nM 3MC, fixed with 4% paraformaldehyde, and permeabilized with 0.5% Triton X-100. Cellular DNA was denatured with 2N HCl. Cells were washed with PBS thrice, blocked with 2% BSA and 0.05% Triton X-100 for 1 h, and stained with BrdU antibody conjugated with alexa-488 (1:500, Life Technologies) for overnight at 4 °C. Nuclei were stained with DAPI and images were captured using C1 confocal microscope (Nikon).

PCR array analysis of skeletal muscle differentiation factors

RT^2 Profiler PCR pathway array (SABiosciences Corporation, Frederick, MD, USA) was used to detect the changes in expression of mouse skeletal muscle differentiation factors [31] using the manufacturer's protocol. Briefly, total RNA from 24 h post 50 nM 3MC or vehicle treated C2C12 myotubes was isolated using an RNeasy mini kit (Qiagen, Hilden, Germany). 1 μg of total RNA was taken for cDNA preparation using random hexamers and the Gene-Amp RNA PCR core kit (Applied Biosystems, Branchburg, NJ, USA), and the resulting cDNA was subjected to the Mouse Skeletal Muscle: Myogenesis & Myopathy (PAMM-099Z) PCR array (SABiosciences). The PCR program included an initial step at 95 °C for 10 min followed by 40 cycles of 15 s at 95 °C for denaturation and 1 min at 60 °C for annealing and extension. The raw data were analyzed using the $\Delta\Delta C_t$ (cycle threshold) method following the manufacturer's web based instructions (SABiosciences).

Samples with a cycle threshold (C_t) of <35 were considered for calculating the fold change in expression. The arithmetic mean of five housekeeping genes was used to normalize the data ($\Delta C_t = C_t$ gene − mean C_t housekeeping). Fold change was calculated using an equation: fold change $= 2^{-\Delta\Delta Ct}$, where $\Delta\Delta C_t = (\Delta C_{tvehicle} - \Delta C_{t3MC})$. Log 10 value of the fold change of each gene was calculated using SABiosciences online web base calculation.

Reverse transcription-PCR

RT-PCR was carried out to validate the expression level of genes associated with differentiation and dedifferentiation [32,33]. The cDNA was amplified by PCR using primers specific to each gene. The PCR program included an initial four cycles of denaturation at 94 °C for 30 s, annealing at 60 °C for 30 s and extension at 72 °C for 45 s, and then 26 cycles of denaturation at 94 °C for 30 s, annealing at 55 °C for 30 s and extension at 72 °C for 45 s for MyoD, Myogenin and GAPDH. And for rest of the genes, PCR program included 30 cycles of denaturation at 94 °C for 30 s, annealing at 55 °C for 30 s and extension at 72 °C for 45 s. Primer sequences of the genes as described earlier [32,33] and the PCR product size are as follows:

Gene name	*Primers (5′-3′)*	*Product size (bp)*
MyoD	For: TACAGTGGCGACTCAGATGC Rev: TAGTAGGCGGTGTCGTAGCC	116
Myogenin	For: AGTGAATGCAACTCCCACAG Rev: ACGATGGACGTAAGGGAGTG	137
Rb	For: CAGGCTTGAGTTTGAAGAAATTG Rev: ATGCCCCAGAGTTCCTTCTTC	168
Anillin	For: GCGTACCAGCAACTTTACCC Rev: GGCACCAAAGCCACTAACAT	202
MRF4	For: GGCTGGATCAGCAAGAGAAG Rev: CCTGCTGGGTGAAGAATGTT	317
M-CK	For: GATCTTCAAGAAGGCTGGTCAC Rev: CAATGATTGGACTTCCAGGAG	428
Cyclin D	For: CCCTTGACTGCCGAGAAGTT Rev: GAAAGTGCGTTGTGCGGTAG	346
Cyclin E1	For: ACTGCATTTCAGCCTCGGAA Rev: GAGCAAGCGCCATCTGTAAC	398
Emi 1	For: ACAGTGGGATAGAAGCTTCC Rev: GCAGCAAGGTTTTGTTGGGA	330
Myf5	For: GAGCGTAGACGCCTGAAGAA Rev: GCTGGACAAGCAATCCAAGC	354
Tubulin	For: CAGAGGGAGCTGAGTTGGTT Rev: AGACGAGATGGTTCAGGTCTC	369
Myh3	For: GGCACATCTCTATGCCACCTT Rev: TCGCAAGCTTTCTTGCTGTC	378
GAPDH	For: GACAACTTTGGCATTGTGGAA Rev: ACACATTGGGGGTAGGAACA	226

GAPDH was used to normalize the amount of cDNA used for PCR. The PCR products were analyzed by 1.8% agarose gel.

Statistical analysis

Data were expressed as the means ± SD. Statistical significance was tested with paired sample *t*-test for means. The differences were considered to be significant if p value was <0.05.

Results

Dedifferentiation of C2C12 myotubes into mononucleated cells

3MC induces tumor formation at the site of injection in the hind leg of mice within 110 days due to the transformation of normal cells to atypical cells [10]. Previously, it has been shown that 3MC could induce dedifferentiation in C2C12 myotubes [11]. To investigate further the mechanism behind the dedifferentiation and to see if mononucleated cells derived from 3MC treated C2C12 myotubes have tumorigenic properties, we first isolated a myotube population from C2C12 myotube cultures which contained mixed populations of single and multinucleated cells. Only isolated myotubes were treated with 3MC or vehicle (DMSO), and time lapse images were captured every 24 h. Fig. 1A shows an example of a 3MC treated myotube (lower panel) that undergoes fragmentation by 48 h whereas a vehicle treated myotube (upper panel) does not show any fragmentation. We tested >100 myotubes in each group, and found that more than 50% of 3MC treated myotubes showed fragmentation to form mononucleated cells whereas approximately 10% of vehicle treated myotubes underwent fragmentation at 48 h (Table 1). Fragmentation is

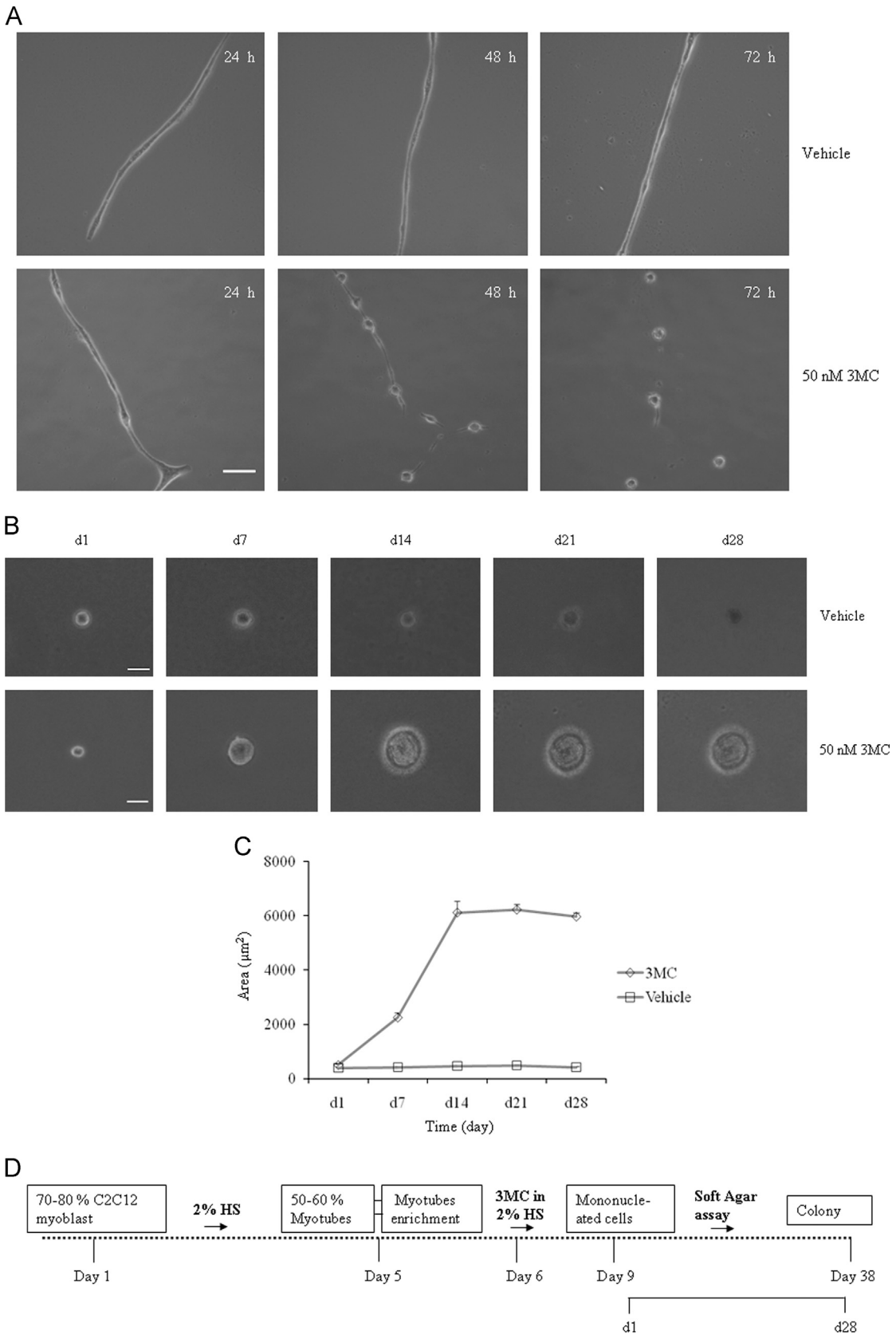

Fig. 1 – 3MC induced mononucleated cells show tumorigenic property. (A) Phase contrast images of vehicle (upper panels) or 50 nM 3MC (lower panels) treated C2C12 myotubes at different time points as indicated. Of note is that the 3MC treated myotube was fragmented by 48 h, but the majority of the vehicle treated myotubes fail to initiate fragmentation and hence multiple mononucleated cells. Scale bar, 100 μm. Time is shown in hour (h). (B) Mononucleated cells were plated on soft agar and allowed to grow. Note that mononucleated cell from 3MC treated myotube (lower panel), but not the vehicle treated myotube (upper panel), shows formation of a colony. Scale bar, 100 μm. Time is shown in day (d). (C) Quantification of area of colonies ($n > 10$) by ImageJ software vs time. (D) Schematic representation of time line for differentiation, addition of drugs and soft agar assay.

thought to be the initial step of dedifferentiation. Other subsequent steps include separation of nuclei and viability of mononucleated cells [34]. Secondly, mononucleated cells were plated on soft agar and allowed to grow. We found that mononucleated cells derived from 3MC treated myotubes formed colonies by day 14 (Fig. 1B, lower panel). We measured the size of colonies ($n>10$) at one week intervals through 4 weeks. Fig. 1C revealed an initial fast growth (till day 14) followed by a saturation. In contrast, neither mononucleated cells derived from vehicle treated myotubes (Fig. 1B, upper panel) nor C2C12 mononucleated myoblasts (Supplemental Fig. S1A) were able to grow in soft agar. These results suggest that 3MC induces fragmentation of C2C12 myotubes and the resulting mononucleates were able to return to the cell cycle and form colonies, which are indicative of cellular dedifferentiation.

Expression profile of myogenic factors and cell cycle regulator in the presence of 3MC during fragmentation

One biochemical indicator of myotube fragmentation would be the reduction in the levels of myogenic differentiation proteins [35,36]. To determine the changes in the expression profile of myogenic factors during fragmentation in the presence of 3MC within 48 h, we performed a myogenic PCR array. We pooled cDNA of three different preparations from each group – 3MC and vehicle treated myotubes. Analysis of array data revealed that none of the myogenic factors in 3MC treated myotubes were expressed more than 2–3 folds over vehicle treated myotubes (Fig. 2A, and Supplemental Tables S1 and S2). We set threshold values +3 and −3, between which is considered negligible change in expression. We validated these findings at the level of RNA by RT-PCR using specific primers and also at the level of protein by immunoblot analysis using antibodies to MyoD and Myogenin, as indicated (Fig. 2B and C). Quantification of the bands of Fig. 2B and C by ImageJ analysis revealed no statistically significant change in the expression of Myogenin or MyoD (data not shown). We also checked genes which are associated with dedifferentiation of myotubes like Rb, Cyclin etc. [33]. Fig. 2D and E show that the expression profile of those genes which remain almost unaltered in the presence of 3MC. We carried out BrdU labeling to determine whether nuclei in the myotubes re-enter into the DNA synthesis phase and investigated the phosphorylation status of Rb at Ser-807/811 for cell cycle progression. Fig. 2F shows that nuclei of 24 h post 3MC treated myotube did not show any BrdU labeling when compared with proliferating myoblasts (Fig. 2G). Supplemental Fig. S3A and B show that a 1.4±0.007 fold increase in the phosphorylation status of Rb at Ser-807/811 in the presence of 20 nM 3MC, but no further increase is seen in the presence of 50 nM 3MC. These results suggest that 3MC is less likely to affect the expression profile of myogenic factors and cell cycle regulators during the fragmentation step of C2C12 myotube's dedifferentiation.

Table 1 – Percentage of myotubes undergo fragmentation in the presence of ML-7, 3MC, or vehicle. Phosphatase inhibitor perturbed the 3MC induced fragmentation of C2C12 myotubes.

	(%) of myotubes fragmented ($n>100$)
Vehicle at 48 h	10±2.5
3MC at 48 h	55±5.5
3MC+phosphatase inhibitors at 48 h	20±3.4
ML-7 at 24 h	45±3.5

3MC induces rearrangement of nonmuscle myosin IIs

Reports on a requirement for NM II in myofibril to accomplish early myofibrillogenesis [12,37] prompted us to check the localization profile of NM IIs in 24 h post 3MC treated myotubes before the fragmentation starts. In control muscle cells i.e. myotubes that were treated with vehicle, NM II-A and -II-B (Fig. 3A and B, left column, shown in arrowheads) were discretely localized in the sarcomere and/or stress fiber in cytosol. However, in the presence of 3MC, both NM IIs were having different localization at the midbody: II-A accumulated at the centre whereas II-B was at the cortex of midbody (Fig. 3A and B, arrows in right column). Both NM II-A and -II-B were co-stained with tubulin in 3MC treated myotubes. Supplemental Fig. S2A–D shows that both NM II-A and -II-B localize at the midbody of fragmented myotubes. These results suggest that fragmentation of multinucleated myotubes could be the outcome of rearrangement of NM IIs.

3MC reduces myosin light chain phosphorylation in C2C12 myotubes

Since NM II localization, activity, assembly, and disassembly are regulated by phosphorylation at Ser-19 of RLC_{20} and/or at non helical domain of the heavy chain, we examined phosphorylation levels in 24 h post 3MC treated myotubes by immunoblot analysis using a phospho specific antibody. Fig. 3C upper panel shows that phosphorylation at Ser-1943 of heavy chain of NM II-A remains unchanged with increasing concentration of 3MC. In contrast, middle panel shows that the amount of RLC_{20} phosphorylation is reduced significantly in the presence of 3MC. Quantification of immunoblots reveals a dose dependent decrease in p-RLC_{20} of 1.4±0.07 fold with 20 nM 3MC and 5.6±0.5 fold with 50 nM 3MC when compared with vehicle treated myotubes (Fig. 3D).

RLC_{20} phosphorylation has been shown to be regulated by both myosin light chain kinase and myosin phosphatase. We inhibited their enzymatic activity using a chemical inhibitor of each of them. Fig. 4A shows that addition of ML-7 (*lane 3*), an inhibitor of myosin light chain kinase, reduces the level of RLC_{20} phosphorylation by 2.6±0.02 fold compared with vehicle (*lane 1*). We tested >100 myotubes from each group and found that ML-7 increased the percentage of myotubes in fragmentation to 45±3.5% (Table 1) at 24 h compared with vehicle treatment which showed only 10±2.5% myotubes in fragmentation at 48 h. We could not continue ML-7 treatment for more than 24 h as after that either fragmented myotubes or mononucleated cells derived from myotubes started detaching from the surface. We also grew the mononucleated cells into soft agar and found that cells were unable to form colonies (Supplemental Fig. S1B). In contrast, when we used a phosphatase inhibitor which inhibited the reduction of RLC_{20} phosphorylation in 3MC treated myotube (Fig. 4A, *lane 2* and 4B), the percentage of myotube fragmentation was reduced to 20±3.4% (Table 1). To analyze the fragmentation step in details, images of myotubes were captured at different time points over 48 h periods in the presence of inhibitors. For this experiment, we tracked myotubes ($n>7$) for each

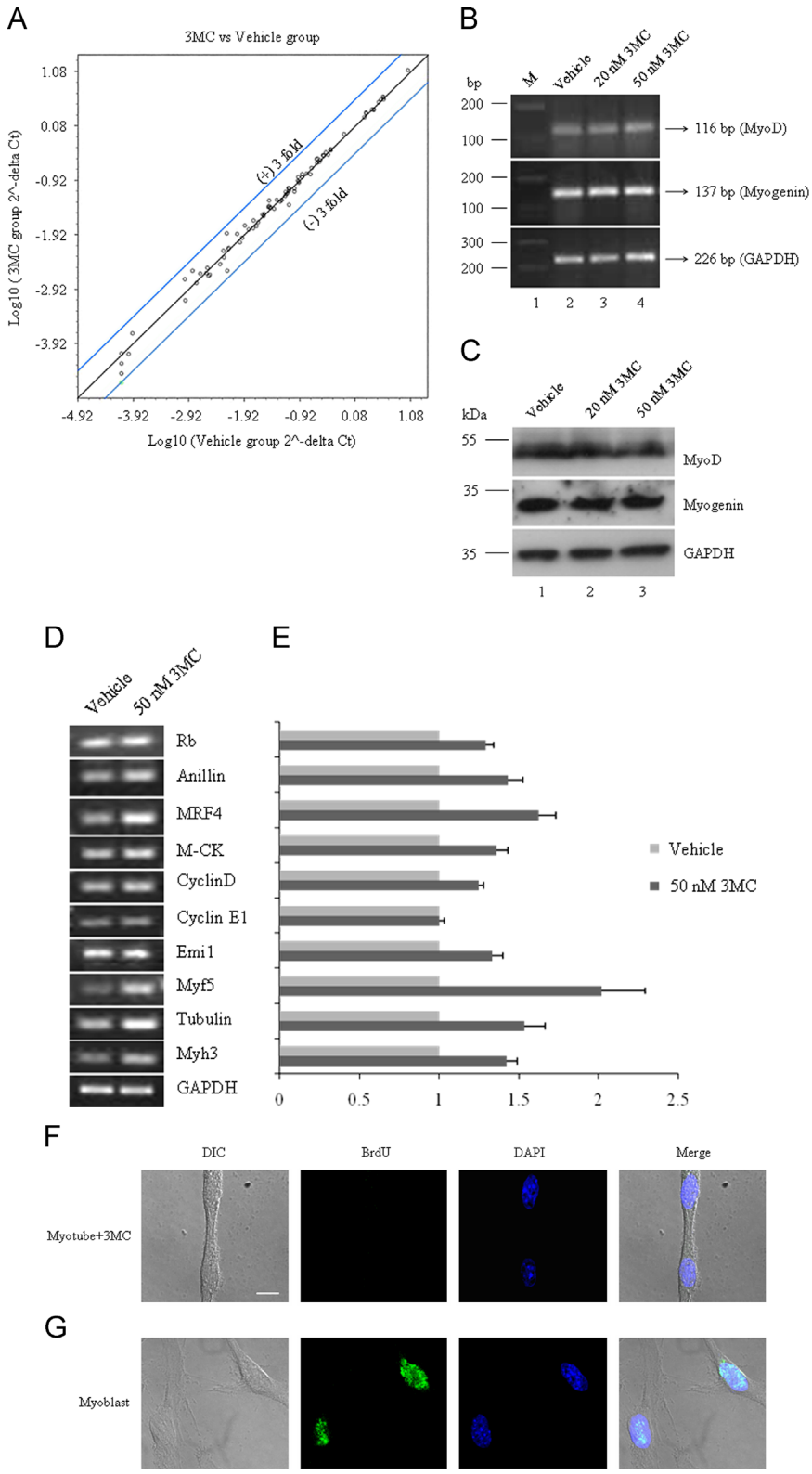

Fig. 2 – Expression profile of genes associated with differentiation and dedifferentiation during fragmentation steps. (A) Scatter plot of myogenic factors from PCR array of vehicle and 50 nM 3MC-treated C2C12 myotubes. Note that none of the factor's position crossed (±) 3 fold lines. (B) RT-PCR analysis of myogenic factors as indicated in the presence of 20 nM 3MC (*lane 3*), 50 nM 3MC (*lane 4*) or vehicle (*lane 2*). GAPDH was used as loading control for cDNA amount. M, DNA size markers (*lane 1*). (C) Cell lysates from vehicle (*lane 1*), 20 nM (*lane 2*), or 50 nM 3MC (*lane 3*) treated myotubes were subjected to immunoblot with antibodies, as indicated. GAPDH was used as loading control. Position of size markers is indicated at left. (D) RT-PCR analysis of genes associated with fragmentation, as indicated, in vehicle and 50 nM 3MC treated myotubes using specific primers. (E) Quantification of bands using Image J analysis. Fold was calculated considering band intensity of vehicle treated myotube as "1". BrdU (green) labeling of 24 h post 50 nM 3MC treated myotube (F) and proliferating myoblasts (G). Proliferating myoblasts were considered as positive control for BrdU-labeling. Nucleus was stained with DAPI. Note that nucleus of 24 h post 3MC treated myotube did not enter into DNA synthesis step. Scale bar, 10 μm.

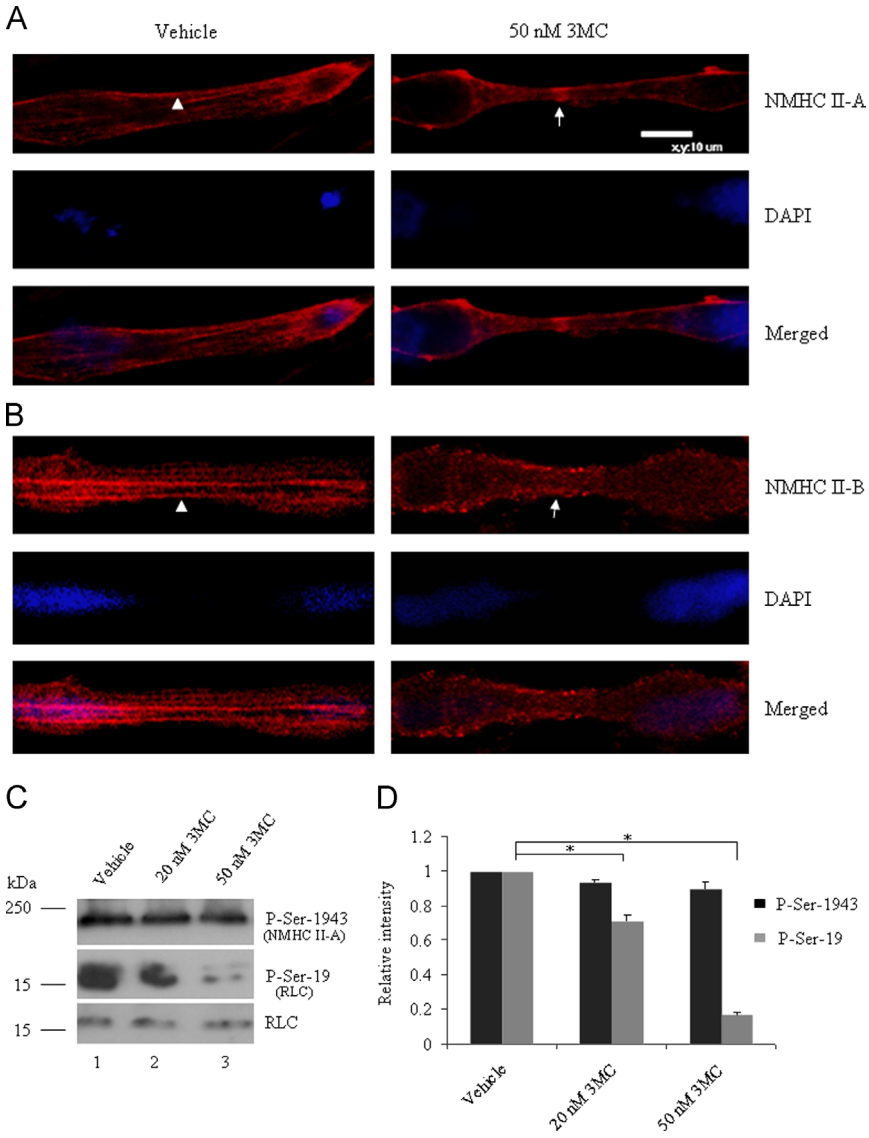

Fig. 3 – Nonmuscle myosin IIs are rearranged during fragmentation. 24 h post vehicle or 50 nM 3MC treated myotubes were fixed, permeabilized and stained with NMHC II-A antibody (A) or NMHC II-B antibody (B). DAPI was used to stain the nuclei. Secondary antibody alexa 594 tagged goat anti-rabbit IgG antibody was used to detect NMHC IIs. Arrowheads in left column show the sarcomeric and/or stress fiber localization of NMHC II-A and -II-B a vehicle treated myotube whereas arrows in right column show the enrichment of NMHC II-A in the center and NMHC II-B in the cortex of the midbody in 3MC treated myotubes. Scale bar, 10 μm. (C) Cell lysates from 24 h post vehicle (*lane 1*), 20 nM (*lane 2*), or 50 nM 3MC (*lane 3*) treated myotubes were subjected to immunoblot with antibodies, as indicated. (D) Quantification of band intensity. Values were expressed considering the relative intensity (p-RLC$_{20}$/RLC$_{20}$ for RLC$_{20}$ or p-Ser 1943/RLC$_{20}$ for heavy chain II-A phosphorylation), of vehicle treated sample as '1'. Results are expressed as mean ± SD from three independent experiments. *$P < 0.05$ for vehicle vs 20 or 50 nM 3MC.

inhibitor. In the presence of ML-7, myotubes started fragmentation after 12 h (Fig. 4C lower panels) compared with vehicle treated myotubes which did not show fragmentation even at 48 h (Fig. 4C, upper panels). In the presence of 3MC alone, myotubes initiated fragmentation after 24 h and within 48 h fragmentation became prominent (Fig. 1A, lower panels). In contrast, addition of phosphatase inhibitor with 3MC did not allow to start fragmentation even at 48 h (Fig. 4C, middle panel). These results, taken together with Fig. 1A and B, strongly suggest that reduction of RLC$_{20}$ phosphorylation during the fragmentation step and carcinogenic property of 3MC are required for dedifferentiation of C2C12 myotubes.

Discussion

Dedifferentiation is an important process by which a terminally differentiated cell can revert back to a less-differentiated stage and is able to proliferate again to replace cells which have been lost during tissue injury [38]. Defining molecular mechanism and factors involved in dedifferentiation in mammals may lead to development of new techniques to control cell and tissue plasticity.

Myoblasts committed to the myogenic lineage can be detected by the expression of Pax3 and MyoD [39]. Activation in a temporal manner of a number of downstream muscle differentiation factors like MyoD, myogenin, myosin heavy chain, troponin T, activated

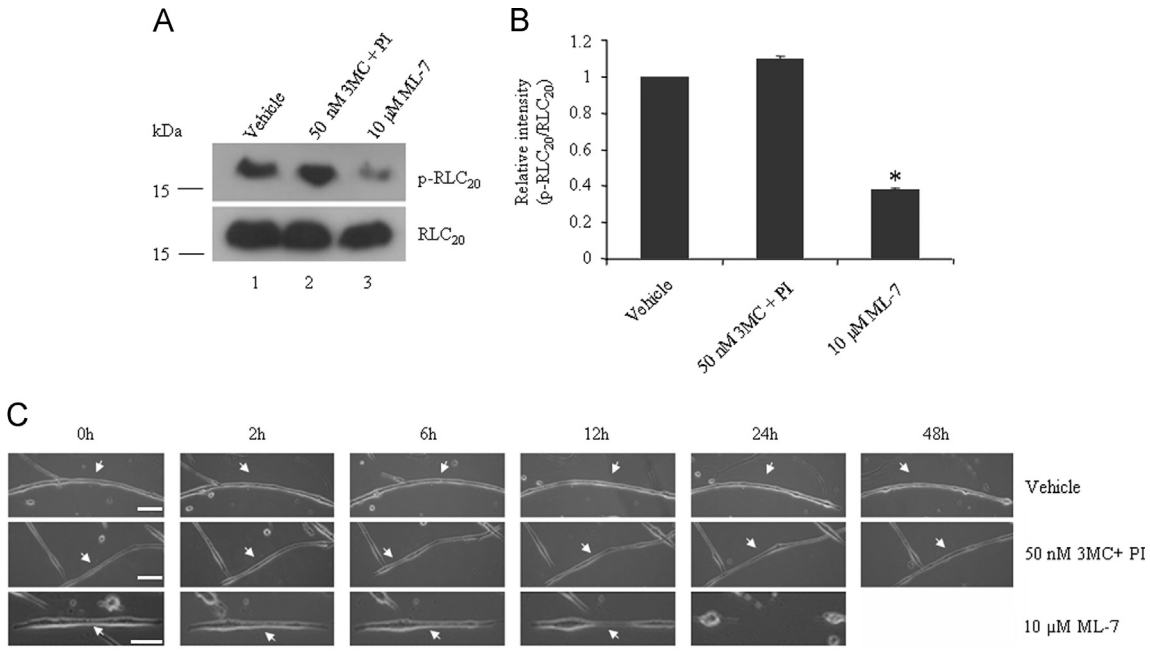

Fig. 4 – ML-7 and phosphatase inhibitors regulate fragmentation of C2C12 myotubes. (A) Cell lysates from 24 h post vehicle (*lane 1*), phosphatase inhibitor with 3MC (*lane 2*) or ML-7 (*lane 3*) treated myotubes were subjected to immunoblot with antibodies, as indicated. (B) Quantification of band intensity. Values were expressed considering the relative intensity (p-RLC$_{20}$/RLC$_{20}$), of vehicle treated sample as '1'. Results are expressed as mean ± SD from three independent experiments. *$P < 0.05$ for vehicle vs ML-7. (C) Time lapse images of C2C12 myotubes treated with vehicle (top panels), phosphatase inhibitor in the presence of 50 nM 3MC (middle panels), or 10 μM ML-7 (bottom panels) at different time points as indicated. Of note is that ML-7 initiates fragmentation by 12 h whereas the phosphatase inhibitor perturbs the fragmentation induced by 3MC. Arrows indicate the myotubes. Time is shown in hour (h). Scale bar, 100 μm.

retinoblastoma protein results in aggregation of the proliferating myoblasts, followed by cell alignment, and fusion of myoblast into linear multinucleated myotubes. At the molecular level, myofibrils begin to form at the cell periphery of the newly fused myotubes from a premyofibril template, whose contractile function is provided by NM II. These initial structures are similar to the stress fibers of motile cells. Additional myofibrils gradually fill the interior of the cell, interconnected with one another and with organelles by desmin rich intermediate filaments. New myoblasts will continue to fuse to the growing ends of the myotube to generate a mature and fully differentiated myofiber, in which mature isoforms of skeletal muscle myosin replace previous NM II [12]. Our data demonstrate that 3MC reduces RLC$_{20}$ phosphorylation and induces rearrangement of NM II location (Fig. 3). We hypothesis that 3MC may be able to reverse the process of myofibril formation without alteration of myogenic factors in 48 h. NM II filament disassembly occurs due to phosphorylation at the non helical domain of the heavy chain and/or dephosphorylation of RLC$_{20}$ [19,40]. Protein kinase C and casein kinase II (CK II) can phosphorylate the heavy chains of myosin II-A and -II-B and reduce their assembly into filaments [41,42]. Elevated level of phosphorylation at Ser-1943 by CK II increased recycling/redistribution of NM II-A in migrating cells [43] and in another study, showed invasive phenotype during epithelial mesenchymal transition by TGF-β signaling pathway [44]. Note that 3MC could reduce the phosphorylation level of RLC$_{20}$ without causing any statistically significant change in heavy chain phosphorylation at Ser-1943 of NMHC II-A (Fig. 3C), suggesting that CK II or TGF-β signaling pathway was less likely affected by 3MC. RLC$_{20}$ phosphorylation can be regulated by myosin light chain kinase (MLCK) or by myosin phosphatase. In our present study, ML-7 a MLCK inhibitor reduced phosphorylation of RLC$_{20}$ while phosphatase inhibitors blocked that reduction, suggesting both MLCK and phosphatase regulated RLC$_{20}$ phosphorylation during dedifferentiation of C2C12 myotubes. We cannot rule out the possibility of other phosphatases which can be involved in RLC$_{20}$ dephosphorylation during 3MC induced dedifferentiation, as the phosphatase inhibitors we used can inhibit more types of phosphatase.

Loss of dedifferentiation is a possible reason for the failure of regeneration in mammals. In urodeles, studies on skeletal muscle suggest that dedifferentiation is a major mode of tissue regeneration. Dedifferentiation involves two independent and separable processes. One is muscle cell fragmentation into individual mononucleated cells and the second is cell cycle re-entry followed by proliferation [34]. Over expression of transcriptional factors such as *msx1* [45], twist [46] or exposure to the small molecule, myoseverin [47], an inhibitor of microtubule assembly causes fragmentation of C2C12 myotubes, and the resultant mononucleated cells are able to proliferate. Pajcini et al. [33] have shown that inhibition of retinoblastoma, Rb, and alternative reading frame, ARF (encoded by *lnk4a* locus), proteins did not cause fragmentation of myotubes but instead induced cell cycle re-entry, suggesting that fragmentation was independent of cell cycle re-entry during dedifferentiation. In our dedifferentiation study, 3MC causes fragmentation within 48 h without changing the expression of myogenic or cell cycle regulatory proteins,

which may support a notion that fragmentation, and regulation of myogenic factors or cell cycle re-entry are independent processes.

We hypothesize that fragmentation, the first step of dedifferentiation, may arise due to loss of cytoskeletal structure. Although mononucleated cells derived from ML-7 treated myotubes are unable to grow in soft agar, further studies are required to determine whether these two processes – fragmentation and proliferation – are interdependent or separate pathways. Our present study shows that a carcinogenic molecule, 3MC, can perform both fragmentation and proliferation. Blocking RLC_{20} dephosphorylation may have a therapeutic application in polycyclic aromatic hydrocarbon induced tumor formation.

Conclusion

Phosphorylation of nonmuscle myosin II regulatory light chain, but not the expression of genes associated with differentiation and cell cycle regulators, is being altered during the fragmentation step in the dedifferentiation of C2C12 myotubes.

Acknowledgments

We thank the Council of Scientific and Industrial Research (CSIR), Government of India (No. 37(1531)/12/EMR-II), and the Indian Association for the Cultivation of Science (IACS) for funding. We thank Dr. Malancha Ta, IISER-Kolkata for her help with the PCR array experiment. SKD and PD thank CSIR, SS and MRD thank IACS for their fellowships.

Appendix A. Supporting information

Supplementary data associated with this article can be found in the online version at http://dx.doi.org/10.1016/j.yexcr.2014.05.015.

REFERENCES

[1] S.R. Kondraganti, P. Fernandez-Saluguero, F.J. Gonzalez, K.S. Ramos, W. Jiang, B. Moorthy, Polycyclic aromatic hydrocarbon-inducible DNA adducts: evidence by 32P-postlabeling and use of knockout mice for AH receptor-independent mechanisms of metabolic activation in vivo, Int. J. Cancer 103 (2003) 5–11.

[2] M. Hollstein, M. Hergenhahn, Q. Yang, H. Bartsch, Z.-Q. Wang, P. Hainaut, New approaches to understanding p53 gene tumor mutation spectra, Mutat. Res. 431 (1999) 199–209.

[3] J.A. Ross, S. Nesnow, Polycyclic aromatic hydrocarbons: correlations between DNA adducts and ras oncogene mutations, Mutat. Res. 424 (1999) 155–166.

[4] D.C. Malins, K.M. Anderson, N.K. Gilman, V.M. Green, E.A. Barker, K.E. Hellstroem, Development of a cancer DNA phenotype prior to tumor formation, Proc. Natl. Acad. Sci. 101 (2004) 10721–10725.

[5] H.W.S. King, M.R. Osborne, P. Brookes, The metabolism and DNA binding of 3-methylcholanthrene, Int. J. Cancer 20 (1977) 564–571.

[6] M.-C. Mathieu, I. Lapierre, K. Brault, M. Raymond, Aromatic hydrocarbon receptor (AhR)·AhR nuclear translocator- and p53-mediated induction of the murine multidrug resistance mdr1 gene by 3-methylcholanthrene and benzo(α)pyrene in hepatoma cells, J. Biol. Chem. 276 (2001) 4819–4827.

[7] M. Naruse, Y. Ishihara, S. Miyagawa-Tomita, A. Koyama, H. Hagiwara, 3-methylcholanthrene, which binds to the arylhydrocarbon receptor, inhibits proliferation and differentiation of osteoblasts in vitro and ossification in vivo, Endocrinology 143 (2002) 3575–3581.

[8] S.R. Kondraganti, K. Muthiah, W. Jiang, R. Barrios, B. Moorthy, Effects of 3-Methylcholanthrene on Gene Expression Profiling in the Rat Using cDNA Microarray Analyses, Chem. Res. Toxicol. 18 (2005) 1634–1641.

[9] L.A. Loeb, C.C. Harris, Advances in chemical carcinogenesis: a historical review and prospective, Cancer Res. 68 (2008) 6863–6872.

[10] C.M. Koebel, W. Vermi, J.B. Swann, N. Zerafa, S.J. Rodig, L.J. Old, M.J. Smyth, R.D. Schreiber, Adaptive immunity maintains occult cancer in an equilibrium state, Nature 450 (2007) 903–907.

[11] S. Saha, S.K. Dey, P. Das, S.S. Jana, Increased expression of nonmuscle myosin IIs is associated with 3MC-induced mouse tumor, FEBS J. 278 (2011) 4025–4034.

[12] J.L. Myhre, B.D. Pilgrim, At the start of the sarcomere: a previously unrecognized role for myosin chaperones and associated proteins during early myofibrillogenesis, Biochem. Res. Int. 2012 (2012) 712315.

[13] N.T. Swailes, M. Colegrave, P.J. Knight, M. Peckham, Non-muscle myosins 2A and 2B drive changes in cell morphology that occur as myoblasts align and fuse, J. Cell Sci. 119 (2006) 3561–3570.

[14] K. Takeda, Z.-X. Yu, S. Qian, T.K. Chin, R.S. Adelstein, V.J. Ferrans, Nonmuscle myosin II localizes to the Z-lines and intercalated discs of cardiac muscle and to the Z-lines of skeletal muscle, Cell Motil. Cytoskelet. 46 (2000) 59–68.

[15] C.L. Moncman, F.H. Andrade, Nonmuscle myosin IIB, a sarcomeric component in the extraocular muscles, Exp. Cell Res. 316 (2010) 1958–1965.

[16] S.S. Jana, S. Kawamoto, R.S. Adelstein, A Specific isoform of nonmuscle myosin II-C is required for cytokinesis in a tumor cell line, J. Biol. Chem. 281 (2006) 24662–24670.

[17] V. Betapudi, L.S. Licate, T.T. Egelhoff, Distinct roles of nonmuscle myosin II isoforms in the regulation of MDA-MB-231 breast cancer cell spreading and migration, Cancer Res. 66 (2006) 4725–4733.

[18] V. Betapudi, V. Rai, J.R. Beach, T. Egelhoff, Novel regulation and dynamics of myosin II activation during epidermal wound responses, Exp. Cell Res. 316 (2010) 980–991.

[19] M. Vicente-Manzanares, X. Ma, R.S. Adelstein, A.R. Horwitz, Non-muscle myosin II takes center stage in cell adhesion and migration, Nat. Rev. Mol. Cell Biol. 10 (2009) 778–790.

[20] L. Gerrits, G.J. Overheul, R.C. Derks, B. Wieringa, W.J. Hendriks, D.G. Wansink, Gene duplication and conversion events shaped three homologous, differentially expressed myosin regulatory light chain (MLC2) genes, Eur. J. Cell Biol. 91 (2012) 629–639.

[21] R.S. Adelstein, M.A. Conti, Phosphorylation of platelet myosin increases actin-activated myosin ATPase activity, Nature 256 (1975) 597–598.

[22] K.E. Kamm, J.T. Stull, Dedicated myosin light chain kinases with diverse cellular functions, J. Biol. Chem. 276 (2001) 4527–4530.

[23] J.C. Sandquist, K.I. Swenson, K.A. DeMali, K. Burridge, A.R. Means, Rho kinase differentially regulates phosphorylation of nonmuscle myosin II isoforms A and B during cell rounding and migration, J. Biol. Chem. 281 (2006) 35873–35883.

[24] D.J. Hartshorne, M. Ito, F. Erdoedi, Role of protein phosphatase type 1 in contractile functions: myosin phosphatase, J. Biol. Chem. 279 (2004) 37211–37214.

[25] M. Frangini, E. Franzolin, F. Chemello, P. Laveder, C. Romualdi, V. Bianchi, C. Rampazzo, Synthesis of mitochondrial DNA precursors during myogenesis, an analysis in purified C2C12 myotubes, J. Biol. Chem. 288 (2013) 5624–5635.

[26] A. Kumar, C.P. Velloso, Y. Imokawa, J.P. Brockes, Plasticity of retrovirus-labelled myotubes in the newt limb regeneration blastema, Dev. Biol. 218 (2000) 125–136.

[27] E.R. Injeti, R.J. Sandoval, J.M. Williams, A.V. Smolensky, L.E. Ford, W.J. Pearce, Maximal stimulation-induced in situ myosin light chain kinase activity is upregulated in fetal compared with adult ovine carotid arteries, Am. J. Physiol. Heart Circ. Physiol. 295 (2008) H2289–2298.
[28] X. Chen, K. Pavlish, J.N. Benoit, Myosin phosphorylation triggers actin polymerization in vascular smooth muscle, Am. J. Physiol. Heart Circ. Physiol. 295 (2008) H2172–2177.
[29] L.J. Wood, J.F. Maher, T.E. Bunton, L.M.S. Resar, The oncogenic properties of the HMG-I gene family, Cancer Res. 60 (2000) 4256–4261.
[30] J.-D. Fang, H.-C. Chou, H.-H. Tung, P.-Y. Huang, S.-L. Lee, Endogenous expression of matriptase in neural progenitor cells promotes cell migration and neuron differentiation, J. Biol. Chem. 286 (2011) 5667–5679.
[31] L.A. Garcia, K.K. King, M.G. Ferrini, K.C. Norris, J.N. Artaza, 1,25 (OH)2 vitamin D3 stimulates myogenic differentiation by inhibiting cell proliferation and modulating the expression of promyogenic growth factors and myostatin in C2C12 skeletal muscle cells, Endocrinology 152 (2011) 2976–2986.
[32] L.C. Hunt, A. Upadhyay, J.A. Jazayeri, E.M. Tudor, J.D. White, Caspase-3, myogenic transcription factors and cell cycle inhibitors are regulated by leukemia inhibitory factor to mediate inhibition of myogenic differentiation, Skelet. Muscle 1 (2011) 17.
[33] K.V. Pajcini, S.Y. Corbel, J. Sage, J.H. Pomerantz, H.M. Blau, Transient inactivation of Rb and ARF yields regenerative cells from postmitotic mammalian muscle, Cell Stem Cell 7 (2010) 198–213.
[34] C.P. Velloso, A. Kumar, E.M. Tanaka, J.P. Brockes, Generation of mononucleate cells from post-mitotic myotubes proceeds in the absence of cell cycle progression, Differentiation 66 (2000) 239–246.
[35] M. Kitzmann, A. Fernandez, Crosstalk between cell cycle regulators and the myogenic factor MyoD in skeletal myoblasts, Cell. Mol. Life Sci. 58 (2001) 571–579.
[36] C.J. McGann, S.J. Odelberg, M.T. Keating, Mammalian myotube dedifferentiation induced by newt regeneration extract, Proc. Natl. Acad. Sci. 98 (2001) 13699–13704.
[37] J.W. Sanger, J. Wang, B. Holloway, A. Du, J.M. Sanger, Myofibrillogenesis in skeletal muscle cells in zebrafish, Cell Motil. Cytoskelet. 66 (2009) 556–566.
[38] C. Jopling, S. Boue, J.C.I. Belmonte, Dedifferentiation, transdifferentiation and reprogramming: three routes to regeneration, Nat. Rev. Mol. Cell Biol. 12 (2011) 79–89.
[39] M. Buckingham, Skeletal muscle progenitor cells and the role of Pax genes, Comptes Rendus Biol. 330 (2007) 530–533.
[40] M.T. Breckenridge, N.G. Dulyaninova, T.T. Egelhoff, Multiple regulatory steps control mammalian nonmuscle myosin II assembly in live cells, Mol. Biol. Cell 20 (2009) 338–347.
[41] N. Murakami, V.P.S. Chauhan, M. Elzinga, Two nonmuscle myosin II heavy chain isoforms expressed in rabbit brains: filament forming properties, the effects of phosphorylation by protein kinase C and casein kinase II, and location of the phosphorylation sites, Biochemistry 37 (1998) 1989–2003.
[42] N.G. Dulyaninova, V.N. Malashkevich, S.C. Almo, A.R. Bresnick, Regulation of myosin-IIA assembly and Mts1 binding by heavy chain phosphorylation, Biochemistry 44 (2005) 6867–6876.
[43] N.G. Dulyaninova, R.P. House, V. Betapudi, A.R. Bresnick, Myosin-IIA heavy-chain phosphorylation regulates the motility of MDA-MB-231 carcinoma cells, Mol. Biol. Cell 18 (2007) 3144–3155.
[44] J.R. Beach, G.S. Hussey, T.E. Miller, A. Chaudhury, P. Patel, J. Monslow, Q. Zheng, R.A. Keri, O. Reizes, A.R. Bresnick, P.H. Howe, T.T. Egelhoff, Myosin II isoform switching mediates invasiveness after TGF-β-induced epithelial-mesenchymal transition, Proc. Natl. Acad. Sci. 108 (2011) 17991–17996.
[45] S.J. Odelberg, A. Kollhoff, M.T. Keating, Dedifferentiation of mammalian myotubes induced by msx1, Cell 103 (2000) 1099–1109.
[46] E. Hjiantoniou, M. Anayasa, P. Nicolaou, I. Bantounas, M. Saito, S. Iseki, J.B. Uney, L.A. Phylactou, Twist induces reversal of myotube formation, Differentiation 76 (2008) 182–192.
[47] O.D. Perez, Y.-T. Chang, G. Rosania, D. Sutherlin, P.G. Schultz, Inhibition and reversal of myogenic differentiation by purine-based microtubule assembly inhibitors, Chem. Biol. 9 (2002) 475–483.